THE JOURNAL OF PHYSICAL CHEMISTRY B

Article

pubs.acs.org/JPCB

Excitons and Excess Electrons in Nanometer Size Molecular Polyoxotitanate Clusters: Electronic Spectra, Exciton Dynamics, and Surface States

Jianhua Bao,[†] Zhihao Yu,[†] Lars Gundlach,[†] Jason B. Benedict,[‡] Philip Coppens,[‡] Hung Cheng Chen,[§] John R. Miller,[§] and Piotr Piotrowiak*,[†]

[†]Department of Chemistry, Rutgers University, Newark, New Jersey 07102, United States

[‡]Department of Chemistry, University at Buffalo, SUNY, Buffalo, New York 14260, United States

[§]Chemistry Department, Brookhaven National Laboratory, Upton, New York 11973, United States

ABSTRACT: The behavior of excitons and excess electrons in the confined space of a molecular polyoxotitanate cluster $Ti_{17}(\mu_4\text{-}O)_4(\mu_3\text{-}O)_{16}(\mu_2\text{-}O)_4(OPr^i)_{20}$ (in short **Ti17**) was studied using femtosecond pump−probe transient absorption, pulse radiolysis, and fluorescence spectroscopy. Due to pronounced quantum size effects, the electronic spectra of the exciton, **Ti17***, and the excess electron carrying radical anion, **Ti17**$^{\bullet-}$, are blue-shifted in comparison with bulk TiO_2 and have maxima at 1.91 and 1.24 eV, respectively. The 0.7 eV difference in the position of the absorption maxima of **Ti17*** and **Ti17**$^{\bullet-}$ indicates the presence of strong Coulomb interaction between the conduction band electron and the valence band hole in the ∼1 nm diameter cluster. Ground state Raman spectra and the vibronic structure of the fluorescence spectrum point to the importance of the interfacial ligand modes in the stabilization and localization of the fully relaxed exciton. Four pentacoordinate Ti sites near the surface of the cluster appear to play a special role in this regard. Solvent polarity has only a minor influence on the spectral behavior of **Ti17***. Exciton recombination in **Ti17** is faster than in anatase nanoparticles or mesoporous films. The kinetics exhibits three components, ranging from less than 1 ps to 100 ps, which are tentatively assigned to the geminate recombination within the core of the cluster and to the decay of the surface stabilized charge transfer exciton. A persistent long-lived component with $\tau > 300$ ps may indicate the involvement of intraband dark states, i.e., triplet excitons ^{3}**Ti17***.

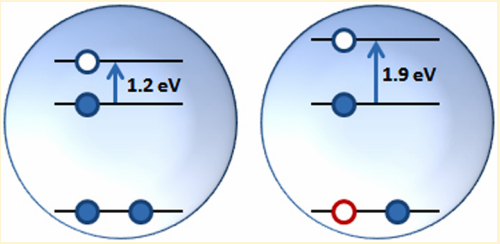

INTRODUCTION

Polyoxotitanate clusters such as the **Ti17** (proper name $(Ti_{17}(\mu_4\text{-}O)_4(\mu_3\text{-}O)_{16}(\mu_2\text{-}O)_4(OPr^i)_{20}$, MW = 2379.46, shown in Figure 1) offer a unique opportunity to investigate quantum size effects in truly homogeneous, monodisperse nanometer size systems. Condensed phase photophysics of such small, well-defined clusters which straddle the boundary between the molecular world and the realm of nanoparticles is virtually unexplored. One of the most intriguing fundamental questions one can ask about these species is to what degree can they be treated as homogeneous core−shell structures, a view illustrated in Figure 1a, and at which point the grainy, atomic structure of the cluster, especially the details of the core−ligand interface and the presence of nonequivalent sites metal sites (Figure 1b), begin to control the exciton dynamics and charge carrier localization.[1−4] Polyoxometalates, most notably the anionic tungstates, molybdates, and vanadates, show promising photocatalytic properties,[5] yet very little is known about the early excited state dynamics in this class of materials.[6] The X-ray structures of several molecular polyoxotitanate clusters were recently determined by Benedict and Coppens[7,8] enabling studies on structure−dynamics correlations at a level that was impossible because of the inherent polydispersity and surface heterogeneity of TiO_2 nanoparticles. Well characterized

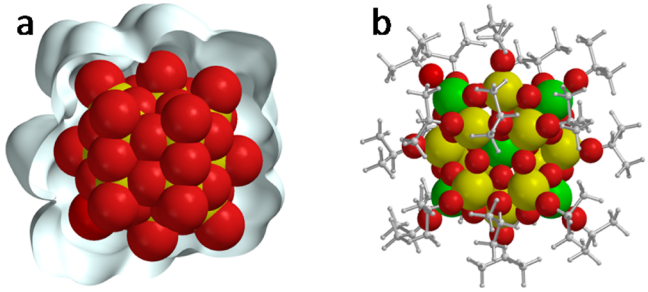

Figure 1. Two representations of the **Ti17** $(Ti_{17}(\mu_4\text{-}O)_4(\mu_3\text{-}O)_{16}(\mu_2\text{-}O)_4(OPr^i)_{20})$ cluster: (a) The homogeneous TiO core immersed in the electron density of the surface isopropoxide ligands with oxygen atoms shown in red and titanium in yellow. (b) A "molecular" view showing the central tetrahedral and the penta-coordinate Ti atoms at the corners of the cluster highlighted in green. For clarity, the radius of the oxygen atoms was reduced, while that of the Ti atoms was exaggerated. The $-C(CH_3)_2$ groups are shown in gray. The Spartan'10 renderings are based on the unrelaxed X-ray structure reported in ref 7.

Special Issue: Paul F. Barbara Memorial Issue

Received: August 3, 2012
Revised: October 26, 2012
Published: October 31, 2012

polyoxotitanate clusters such as that described here **Ti17** can serve as very attractive, experimentally and theoretically tractable models for colloidal TiO_2, the most widely studied wide band gap semiconductor substrate for hybrid photovoltaic materials[9] and a potent photocatalyst for hydrogen production[10] and pollutant remediation.[11]

In this paper, we report the results of combined laser pump–probe and pulse radiolysis experiments aimed at the understanding of the exciton dynamics, charge localization, and electron–hole coupling in the **Ti17** cluster. Optical excitation of **Ti17** generates **Ti17*** excitons, i.e., electron–hole pairs in which the charges interact with one another, while pulse radiolysis places a single excess electron in the lowest empty orbital (LUMO) or the conduction band (CB) of the cluster, leading to the formation of the corresponding radical anion, **Ti17**$^{\bullet-}$. In the case of a single excess charge, the confinement affects only the quantized kinetic energy of the electron, while for the exciton the kinetic, Coulomb, and exchange energy are all affected by the size of the nanoparticle.[1−3] The combination of pulse radiolysis and optical spectroscopy gives a more complete view of the electronic states of **Ti17** and allows a better grasp of the electron–hole interaction in the confined volume of the cluster.

The crystallographic structure of the polyoxotitanate core of **Ti17** resembles most closely brookite, the least common metastable phase of crystalline TiO_2.[7] The core of the cluster is terminated by 20 isopropoxide groups (Figure 1b). As a result, the outer shell of the cluster is for the most part hydrophobic, resulting in good solubility in even mildly polar organic solvents. There are four five-coordinate titanium ions which form a square centered around the unique tetrahedral Ti ion positioned in the middle of the cluster (shown in green in Figure 1b). The remaining 12 Ti ions have the most typical, 6-fold coordination. The system has an approximate S_4 rather than spherical symmetry, and there is considerable disorder in the orientation of the isopropyl groups. As it will be seen, the existence of nonequivalent and coordinatively unsaturated Ti sites has a significant influence on the electronic properties of the cluster.

Because titanium dioxide is a large band gap II–VI semiconductor with a strong ionic character,[18,19] the onset of quantum size effects is expected to occur for much smaller particles than in the case of chalcogenides and other small band gap covalent solids. Serpone et al. concluded that quantum size effects were not significant in anatase particles down to ∼2.1 nm diameter, which corresponds to approximately 200 Ti atoms;[20] however, the oxotitanate core of **Ti17** contains only 17 Ti atoms and is approximately 10 times smaller by volume. Its furthest Ti centers span 8.3 Å, and the maximum distance between the surface oxygen atoms is 11.4 Å. At these dimensions, quantum confinement effects are clearly manifested in the ground state electronic absorption spectrum of **Ti17**. The line shape analysis performed by Benedict and Coppens placed the band edge of **Ti17** at 4.3 eV (∼290 nm) and the lowest indirect transition at 3.4 eV (∼365 nm).[7] For comparison, the band gaps of bulk anatase, rutile, and brookite are 3.2, 3.0, and 3.3 eV, respectively (Table 1).

We have found that the small size of the cluster has an even more dramatic influence on the spectral properties of **Ti17*** and **Ti17**$^{\bullet-}$ than on the ground state absorption. In bulk semiconductors and large nanoparticles, excitons can dissociate and form free carriers. In rutile, the exciton binding energy is as small as 4 meV, and in anatase, it is believed to be larger, on the

Table 1. Key Photophysical Parameters of Rutile, Anatase, Brookite, and the Ti17 Cluster[7,11−17]

	Ti17 cluster	brookite	anatase	rutile
direct band gap (eV)	4.3	3.4	3.7	4.2
indirect band gap (eV)	3.36	3.27	3.24	3.03
fluorescence origin (eV)	3.36	N.A.	3.85	3.03
λ_{max} e^- (nm)	1000	N.A.	>10 000	>10 000
λ_{max} $\{e^-, h^+\}$ (nm)	650	N.A.	>3000	>3000
phonon frequency (cm^{-1})	644, 592, 550	635, 585, 535	639	609

order of 20 meV, i.e., still approximately only 1 k_BT.[18,19] In the case of **Ti17**, because of the confinement, the charges remain strongly coupled to one another and cannot fully dissociate. Classical Coulomb interaction calculated at the maximum electron–hole separation permitted by the 1 nm diameter of the TiO core of the cluster is approximately 250 meV, i.e., equivalent to 10 k_BT at room temperature. Better estimates can be obtained using Brus type expressions[2−4] which account for the electron–phonon and hole–phonon coupling (nuclear reorganization in the molecular terminilogy) by introducing an adjustable effective mass for both charges; however, since these parameters are not known for the cluster, we will use the rough value of 0.25 eV as a convenient zeroth-order reference point.

The results reported here show that the simple core–shell picture presented in Figure 1a cannot fully account for the behavior of **Ti17** and that a molecular view of the cluster is more appropriate. We propose tentative energy level diagrams for **Ti17** and **Ti17**$^{\bullet-}$ radical anion shown in Figure 2. Because

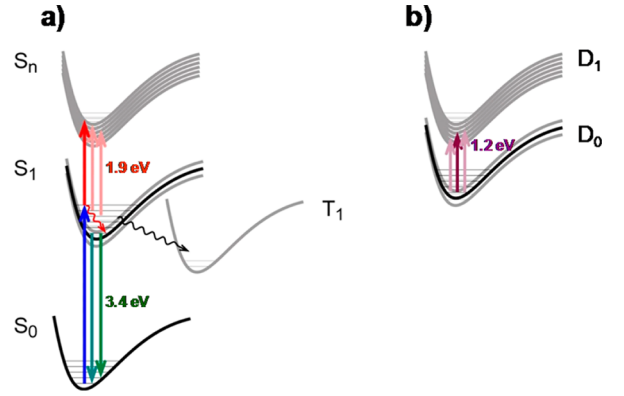

Figure 2. Tentative energy level diagrams of: (a) The neutral **Ti17** polyoxotitanate cluster and (b) the **Ti17**$^{\bullet-}$ reduced species carrying the excess electron.

of the strong electron–hole coupling, the absorption spectrum of the exciton is shifted to a much higher frequency than in bulk TiO_2 (Table 1 and Figure 3). The broad spectra of **Ti17**$^{\bullet-}$ and **Ti17*** are consistent with a sequence of closely lying higher electronic states, S_n and D_n, respectively, which are shown as gray lines in Figure 2. The existence of the T_1 triplet is inferred from the multicomponent charge recombination dynamics and from the large magnitude of the electron–hole coupling, which suggests there is sizable exchange interaction in the **Ti17*** excited state. The fluorescence and Raman spectra indicate that the atomic-level structure of the core–shell interface and the vibrational modes of the ligands play a very important role in stabilizing the S_1 excited state. The presence of large gaps between the lowest S_1 excited state and the manifold of S_n

dx.doi.org/10.1021/jp307724v | J. Phys. Chem. B 2013, 117, 4422−4430

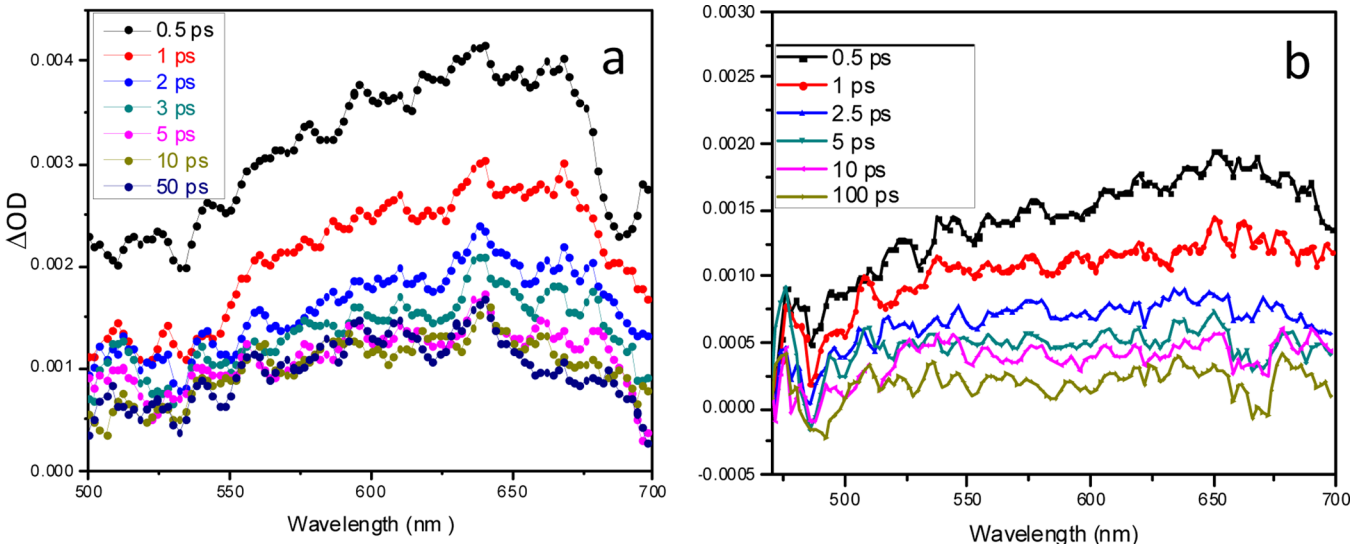

Figure 3. Femtosecond pump–probe transient absorption spectra of the **Ti17*** excited state in (a) benzonitrile, ε = 25.6; (b) dibutyl ether, ε = 4.3.

states as well as between the D_0 ground state and the D_n manifold of doublets is not consistent with the bulk-like picture of **Ti17**. We postulate that the S_1 and D_0 states are rather tightly localized and stabilized by nuclear reorganization at the core–ligand interface, while the higher, densely spaced S_n and D_n states involve primarily the orbitals of the polyoxotitanate core and hence are of a more bulk-like character.

In the body of the paper, we will continue to apply **Ti17*** as a general symbol for the **Ti17** excited state or exciton, while the S_1, S_n, and T_1 terms will be used when more precise labels are necessary for clarity.

EXPERIMENTAL METHODS

Synthesis. The synthesis, purification, and structural characterization of the **Ti17** polyoxotitanate clusters were described in detail in the literature.[7,21,22]

Sample Preparation. Benzonitrile (Acros) and dibutyl ether (Sigma-Aldrich) were dried on 4 Å molecule sieves and used without further purification. Samples for the transient absorption measurements were prepared by dissolving approximately 3 mg of solid **Ti17** in 2 mL of dry solvent. After 30 min, the clear solution was transferred into a standard quartz cuvette with an airtight valve. The entire process was carried out in a glovebox.

Steady-State Spectroscopy. Absorption spectra were measured with a Varian Cary 500 spectrometer. Fluorescence spectra were recorded on a Varian Cary Eclipse fluorimeter (resolution 2.5 nm).

Raman Microspectroscopy. Approximately 1 mg of the **Ti17** or **Ti17cat4** cluster was spread in an indentation in a clean brass cell and covered by a glass slide with vacuum oil along the edge to prevent air from entering the sample. Sample preparation was carried out in a glovebox. Raman spectra were acquired using a Kaiser Optical Systems Confocal Raman Microprobe equipped with a 785 nm diode laser. A 100× oil immersion objective was used to focus approximately 6–10 mW of the single mode power within the sample volume of ~2 μm^3. The spectral coverage ranged from 100 to 3450 cm^{-1}, and the resolution was 4 cm^{-1}. The spectra were acquired using 4 accumulations of 60 s exposure time each.

Pump–Probe Transient Absorption Spectroscopy in the Visible and IR. 70 fs pulses at 795 nm were provided by a home-built 1.25 kHz multipass Ti:sapphire amplifier seeded by a Spectra-Physics Tsunami oscillator. The output of the amplifier was split to generate independently tunable pump and probe pulses. The pump beam (~25 fs, 3.5 mW, 300 nm) was produced by frequency doubling the output of a noncollinear optical parametric amplifier (Topas White, Light Conversion). The pump was modulated at 17 Hz with the help of a mechanical chopper. The probe beam was delayed with respect to the pump using a computer-controlled delay stage and focused into a 2 mm sapphire plate to generate white light continuum. The white light was overlapped with the pump beam in a 10 mm fused silica cuvette containing the sample. The probe light was dispersed with a monochromator (Oriel MS257 with a 1200 lines/mm grating) and detected with a Si photodiode (Thorlabs, DET110). The absorption spectra were collected in the lock-in mode (Stanford Research, SR 810) with the monochromator scanning the wavelength range and the pump–probe delay fixed at the desired value. The relative polarization of the pump and probe beams was set at the "magic angle".

The IR transients were obtained using as a probe sub-100 fs pulses produced by a home-built IR OPA based on parametric down-conversion in $KNbO_3$ and pumped by the same multipass Ti:sapphire amplifier as above. In order to optimize the relative duty cycles, the output of the IR detector (InAs photodiode) was sampled with a boxcar integrator (Stanford Research 280) the analog output of which served as the input for the lock-in amplifier. Instead of using IR interference filters, we took advantage of the narrow transparency window of acetonitrile at 2.65 μm to select the desired wavelength. The **Ti17** sample was prepared in the same fashion as described above. The anatase film on a thin silica substrate was prepared as described in the literature.[23] It was placed in a cuvette containing acetonitrile in order to ensure comparable experimental conditions.

Pulse Radiolysis. The spectra of $\mathbf{Ti17}^{\bullet-}$ were obtained at the Laser-Electron Accelerator Facility (LEAF) at the Brookhaven National Laboratory. LEAF and the methods used are described elsewhere.[24] Briefly, an electron pulse (≤120 ps duration) was focused into a quartz cell with an optical path

dx.doi.org/10.1021/jp307724v | J. Phys. Chem. B 2013, 117, 4422–4430

length of 20 mm containing the solution of interest. The monitoring light source was a 65 W xenon arc lamp pulsed to a few hundred times its normal intensity. Wavelengths were selected using 10 nm bandpass interference filters. Transient absorption signals were detected with either an FND-100Q silicon diode ($\lambda \leq 1000$ nm, 2 ns, EG&G) or a GAP-500L InGaAs diode ($\lambda \geq 1100$ nm, 8 ns, Germanium Power Devices) and digitized with a Tektronix TDS-680B or a LeCroy 8420A oscilloscope. The electron pulses ionized the solvent, benzonitrile, to produce its anions and cations. Electrons from the solvent anions ("excess electrons") were transferred to **Ti17**, reducing it and producing **Ti17**$^{\bullet-}$, i.e., the radical anion of the cluster. Benzonitrile cations cannot oxidize **Ti17**, and as a result, the corresponding **Ti17**$^{\bullet+}$ species was not observed. This was confirmed by experiments on **Ti17** solutions saturated with SF_6, which selectively scavenges the excess electrons. Under these conditions, neither **Ti17**$^{\bullet+}$ nor **Ti17**$^{\bullet-}$ were observed.

Computation. The calculation of the Raman and IR absorption spectra of the isopropoxide anion and the oxo isopropoxyl radical was carried out at the DFT B3LYP level with the 6-31G* basis set using the Spartan'10 software package by Wavefunction, Inc. The resulting vibrational frequencies were not scaled.

RESULTS AND DISCUSSION

Excitation of **Ti17** with 300 nm ~25 fs pulses results in the formation of the S_1 excited state which is characterized by a broad and featureless spectrum which spans nearly the entire visible range from 500 to 750 nm (Figure 3). The large spectral width, lack of structure, and gradual falloff on the high energy side are consistent with a closely spaced sequence of higher electronic excited states of the cluster (Figure 2). The transitions to the closely lying S_2, ..., S_n electronic states have diminishing oscillator strength and suggest the onset of continuum (ionization of the **Ti17*** excited state) at around 2.5 eV. The spectra in two solvents, dibutyl ether and benzonitrile, which differ considerably in polarity (ε = 4.3 for the former and ε = 25.6 for the latter), are nearly indistinguishable from one another. The spectrum in dibutyl ether does appear to be somewhat broader and possibly slightly red-shifted; however, even in the presence of these minor differences, one must conclude that the influence of solvent polarity on the spectrum of **Ti17*** is small. This suggests that the isopropoxide ligands, which form a dense cover on the surface of the cluster, reduce the solvation effects by shielding the core of the cluster from the surrounding medium. In essence, the ligands themselves act as the first solvation shell for the exciton and diminish the polarization of the bulk solvent. Alternatively, such weak solvent dependence could indicate that the relaxed S_1 state has little CT character and that the electron and the hole are not spatially well separated. This explanation is unlikely given the presence of nonequivalent Ti centers and the ionic nature of the TiO core.

The 650 nm (1.9 eV) maximum of the **Ti17*** spectrum lies at a much higher energy than that for the bulk exciton or conduction band electron in TiO_2, which also has a very broad and featureless spectrum with λ_{max} > 10 000 nm, i.e., <0.1 eV.[17,25] This dramatic blue shift of more than 1.8 eV points to the presence of strong quantum size effects and increased electron–hole coupling in the 1 nm cluster, as discussed in the Introduction. In order to confirm that **Ti17*** does not have lower-lying electronic transitions, we also probed the response of the directly excited cluster and anatase in the near IR (1200–

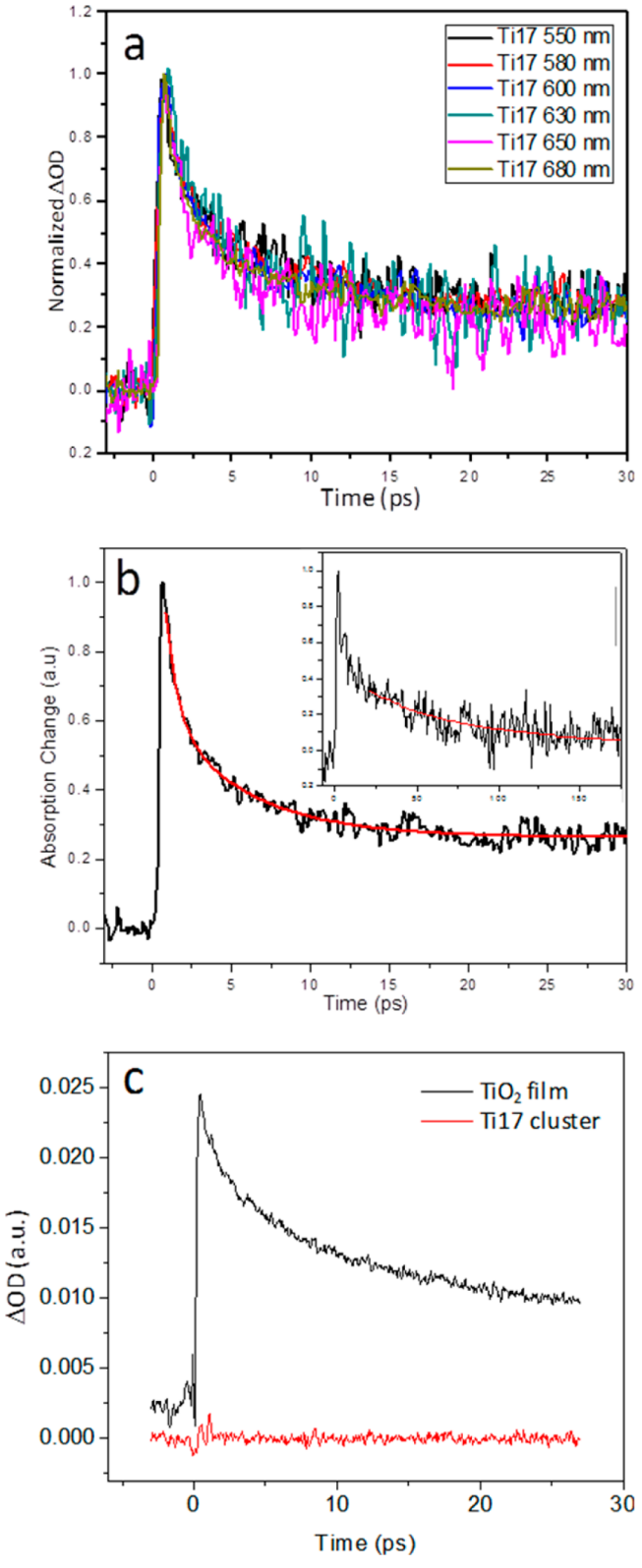

Figure 4. (a) Overlayed normalized transients collected at several wavelengths from 550 to 680 nm showing homogeneous decay kinetics. (b) Decay of the excited state of **Ti17** in dibutyl ether monitored at 680 nm (excitation at 300 nm) fitted with a biexponential function with τ_1 = 0.75 ps and τ_2 = 5.3 ps. A longer time scale decay fitted with τ_3 = 102 ps is shown in the inset. (c) IR transient responses of the **Ti17** cluster (red) and anatase film (black) probed at 2.65 μm.

dx.doi.org/10.1021/jp307724v | J. Phys. Chem. B 2013, 117, 4422–4430

Table 2. Exciton Decay Parameters Measured for Ti17 in Dibutyl Ether, Excitation at 300 nm

τ_1 (ps)	A_1	τ_2 (ps)	A_2	τ_3 (ps)	A_3	A_∞
0.75 ± 0.2	0.31 ± 0.06	5.3 ± 0.8	0.34 ± 0.04	102 ± 18	0.28 ± 0.04	0.07 ± 0.05

1400 nm) and IR (2650 nm) spectral regions. The resulting transients obtained for **Ti17** and a mesoporous TiO_2 film at 2.65 μm are shown in Figure 4c. The directly excited TiO_2 film shows at this wavelength strong absorption in agreement with the findings of Katoh et al.;[25] however, the only signal that we were able to detect in the case of **Ti17** is the small nonlinear artifact at t = 0. This verifies that **Ti17*** has no low-lying allowed electronic transitions below the 700 nm. It should be mentioned that photoexcited **Ti17**, unlike rutile or anatase, does not give a response in the terahertz frequency range.[26] The lack of IR and terahertz absorption corroborates the presence of strong electron−hole coupling in **Ti17*** and suggests that the cluster does not have a true conduction band. It is more likely that the appearance of the spectrum of **Ti17*** is due to a sequence of closely spaced localized and delocalized d−d transitions in the core of the cluster.

Exciton Relaxation and Recombination Dynamics. The broad transient absorption spectra of the **Ti17*** excited state decay homogeneously, as shown in Figures 3 and 4a. While there appears to be a barely perceptible shift to the blue during the initia1 1 ps following the excitation, the low signal-to-noise ratio of the available data, combined with the large width of the spectrum, do not justify a more detailed analysis of the spectral dynamics. Similarly to the **Ti17*** absorption spectrum, its decay dynamics is weakly dependent on solvent polarity and the systematic differences between the benzonitrile and dibutyl ether results were smaller than the fitting uncertainties. This further supports the picture of an exciton shielded from the solvent by the ligand shell.

The kinetics in the 0−30 ps time window, which was examined most extensively in this work, is dominated by two components, τ_1 = 0.75 ps and τ_2 = 5.3 ps, which together constitute more than 60% of the overall decay (Figure 3b and Table 2). Since the pump−probe data were collected in the "magic angle" configuration and since the spectral evolution is minor, these rates reflect purely the population decay. The fastest subpicosecond rate most likely corresponds to the geminate recombination of the initial electron−hole pairs which did not fully equilibrate with the 550−640 cm^{-1} phonon modes of the TiO core of the cluster (Table 1). The surviving excitons follow two paths: they either decay with the rate τ_2, which is consistent with vibrational cooling, or acquire charge transfer character with one of the charges stabilized at the core−ligand interface, consistent with the view that in small nanocrystallites the interaction with the surface dominates the electron and hole dynamics.[1] Skinner et al. found that in colloidal TiO_2 the electron localizes within a picosecond on coordinatively unsaturated Ti centers,[27] which in the case of **Ti17*** suggests the central tetrahedral Ti atom (Figure 1b) as the location of the negative charge in the relaxed excited state. The crucial involvement of surface states in stabilizing the hole is elaborated in more detail in the following sections of the paper. Longer scans up to 300 ps (Figure 4b, Table 2) allowed us to determine the third decay time, τ_3 = 102 ps, which we ascribe to the recombination of the fully relaxed, surface-stabilized exciton. Only less than 30% of the initial excited state population reaches this stage.

Lastly, fitting of the long scan transients always returned a 5−10% A_∞ component which does not decay at the 300 ps time scale. While we cannot rule out the presence of small amounts of impurities or photodamage of the cluster itself, even though precautions were taken to minimize the latter, it is plausible that the longest lived absorption component originates from the "dark" intraband states, i.e., triplet excitons ^{3}**Ti17***, or in the molecular terminology, simply the T_1 triplet state of the cluster (Figure 2). As it will be shown below, the electron−hole coupling in the confined space of **Ti17** appears to be large, on the order of 6000 cm^{-1} or 30 k_BT. This coupling consists of the Coulomb and exchange interaction, the latter of which leads to the singlet−triplet splitting of the excited state. One cannot easily determine the partitioning of the overall interaction into the Coulomb and exchange components. However, if the S−T splitting is larger than k_BT, which it is very likely to be given the large magnitude of the overall electron−hole interaction, a distinct, slower recombination dynamics of the triplet exciton should be expected. A definitive proof of the existence of such triplet states would be to detect low temperature phosphorescence of **Ti17**. These efforts are under way.

Spectrum of the Excess Electron and the Electron−Hole Coupling in the Excited State of Ti17. In bulk semiconductors, the direct electron−hole coupling is small. As mentioned earlier, the exciton binding is only 4 meV in rutile and 20 meV in anatase.[18,19] These values contain both the direct electrostatic interaction and the lattice relaxation (phonon trapping) effects. Because the perturbation is small, the absorption spectra of the exciton and the free conduction band electron are usually very similar to one another. Furthermore, at room temperature, the exciton rapidly dissociates into free carriers. In the case of a ∼1 nm diameter particle such as the **Ti17** cluster, even if the phonon (nuclear reorganization) effects were negligible, the two charges cannot migrate far from one another. Since the exciton in **Ti17** cannot fully dissociate, the electron and the hole remain coupled by the large Coulomb interaction and the absorption spectra of **Ti17*** and **Ti17**$^{\bullet-}$ should differ markedly. For this reason, independent spectral characterization of the **Ti17**$^{\bullet-}$ radical anion is very important if one wishes to understand the behavior of the quantum confined excess electron in the absence and presence of the electrostatic perturbation exerted by the hole. The comparison of the absorption spectra of **Ti17**$^{\bullet-}$ and **Ti17*** offers insights into the interplay between the pure "particle-in-the-box" confinement which in the zeroth-order approximation affects only the kinetic energy of the excess electron in **Ti17**$^{\bullet-}$ and the Coulomb and exchange interactions, which are also modified by the restricted space available to the electron−hole pair in **Ti17***.[2−4]

After several unsatisfactory attempts to generate sufficient concentrations of **Ti17**$^{\bullet-}$ electrochemically, we turned to fast pulse radiolysis, which is ideally suited for the study of challenging metastable redox intermediates (see the Experimental Methods section for more details). The resulting spectrum of e^- in the "conduction band", or the lowest unoccupied orbital of the cluster, is shown in Figure 5a. The broad and highly asymmetric absorption band of the excess electron appears at a much longer wavelength than the

dx.doi.org/10.1021/jp307724v | J. Phys. Chem. B 2013, 117, 4422−4430

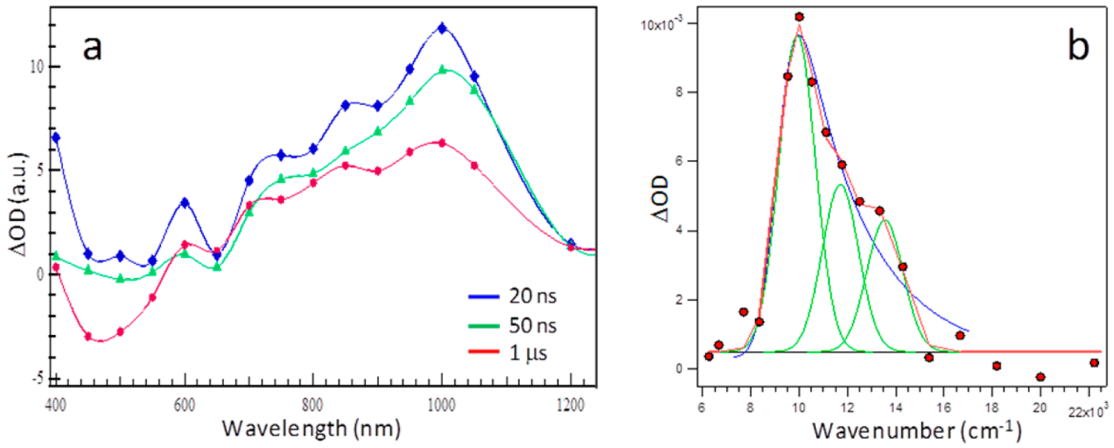

Figure 5. (a) Absorption spectra of the **Ti17**$^{\bullet-}$ species at different delay times obtained by picosecond pulse radiolysis in benzonitrile. (b) Gaussian (green) and stretched Gaussian (blue) line shape fitting of the **Ti17**$^{\bullet-}$ absorption band obtained at 50 ns delay. The solid red line is the sum of the three Gaussian functions calculated only at the frequencies of the experimental data.

spectrum of **Ti17***. The absorption maximum lies at 1000 nm (1.24 eV), i.e.,1.1 eV higher than that of the conduction band electron in bulk TiO_2 and 0.67 eV lower than that of the **Ti17*** exciton, simultaneously confirming the presence of pronounced quantum size effects in **Ti17**$^{\bullet-}$ and strong electrostatic interaction between the electron and the hole in **Ti17***. The rise on the low energy side is very sharp, while the high energy falloff is much more gradual. The spectrum cannot be satisfactorily fitted with a single Gaussian or Lorentzian line shape; however, a sequence of three 1900 cm^{-1} wide Gaussian peaks centered at 9920, 11 710, and 13 550 cm^{-1} reproduces it perfectly (Figure 5b, green lines). Given the low resolution of the experimental spectrum, one should be prudent not to overinterpret the origin of the modulation seen in Figure 5a. Indeed, a single Gaussian convoluted with an exponential function gives a very satisfactory fit, too (Figure 5b, blue line). Nonetheless, the asymmetric shape of the band alone indicates that it consists of a sequence of transitions to a series of closely spaced higher states with diminishing oscillator strength, similarly as the spectrum of **Ti17***, albeit shifted to lower energy. It is more likely that these are closely lying higher electronic doublet states D_2, ..., D_n shown in Figure 2 rather than a vibronic progression of the same electronic transition. Indeed, the apparent ~1800 cm^{-1} separation between the features does not correspond to any vibrational mode of the TiO core or the ligands. In the future, we will attempt to obtain better resolved spectra of **Ti17**$^{\bullet-}$ and address this point in more detail.

The 0.67 eV shift between the spectra of **Ti17**$^{\bullet-}$ and **Ti17*** can be used to set a rough limit for the electron−hole distance in the relaxed excited state of **Ti17**. In a vacuum, 0.67 eV corresponds to the potential energy of two point charges separated by ~2.1 nm, i.e., further apart than both the diameter of the TiO core and the size of the entire **Ti17** cluster. Scaled by the high frequency dielectric constant of anatase, $\varepsilon_{opt} \approx 6$, the estimated electron−hole separation is reduced to $r_{+-} = 0.35$ nm. This value is nearly identical with the 3.50 Å distance between the central tetrahedral and the outer, six-coordinate Ti atoms and it is only slightly shorter than the 4.2 Å distance between the center of the cluster and the five-coordinate Ti atoms based on the X-ray diffraction structure determination.[7] Such crude classical electrostatic estimates ignore the atomic structure of the medium, charge delocalization, as well as exchange interactions and should be taken with caution. Even the use of the bulk dielectric constant of anatase is questionable, since it is has been convincingly argued that in nanoparticles the effective ε is lower.[28] Nevertheless, they suggest that the relaxed exciton in **Ti17** has substantial charge-separated character, most likely with the electron occupying the terahedral center of the cluster and the hole localized at the electron-rich Ti−isopropoxide interface between the core and the ligand shell. The emerging picture of a charge transfer excited state and the involvement of the ligand−core interface are corroborated by the fluorescence and Raman spectroscopy results discussed in the next section. Excited states of other polyoxometalates (POMs), e.g., the $[W_{10}O_{32}]^{4-}$, are also believed to be of the LMCT (ligand-to-metal charge-transfer) character, with the electron residing at one of the metal centers.[6] Furthermore, in colloidal TiO_2, the conduction band electron localizes on the coordinatively unsaturated Ti ions.[27]

The large Coulomb interaction in the excited state of **Ti17** suggests that the exchange coupling K between the unpaired HOMO−LUMO (or valence band−conduction band) electrons is also substantial in this system. As mentioned earlier, the 0.67 eV spectral shift observed for the **Ti17*** exciton in comparison with the **Ti17**$^{\bullet-}$ radical anion is a composite result of both interactions. Exchange interaction K raises the energy of the singlet exciton by K and lowers the energy of the otherwise degenerate triplet state by the same amount. Coulomb and exchange integrals have different distance dependence, with the short-range part of the latter scaling as the inverse of the common volume sampled by the unpaired spins.[29−31] If we accept the 2.35 nm Bohr radius of the free exciton in anatase deduced recently by Hormann et al.[32] and combine it with the particle size dependence of the electron−hole exchange energy derived by Takagahara,[29] an over 100-fold increase in the exchange interaction is predicted for the **Ti17** cluster in comparison with bulk anatase TiO_2. For a reference, in the case of the fully delocalized π-electron system of C_{60}, which is similar in size to **Ti17**, the singlet−triplet splitting is on the order of 0.3−0.4 eV.[33,34] Naturally, any localization of the hole and the electron away from one another through charge separation or phonon coupling, both of which certainly take place in **Ti17***, will affect these values. Nevertheless, as long as the singlet−triplet splitting remains greater than the thermal energy, $E_{S-T} = 2|K| > k_BT$, it is likely to manifest itself in the

dx.doi.org/10.1021/jp307724v | J. Phys. Chem. B 2013, 117, 4422−4430

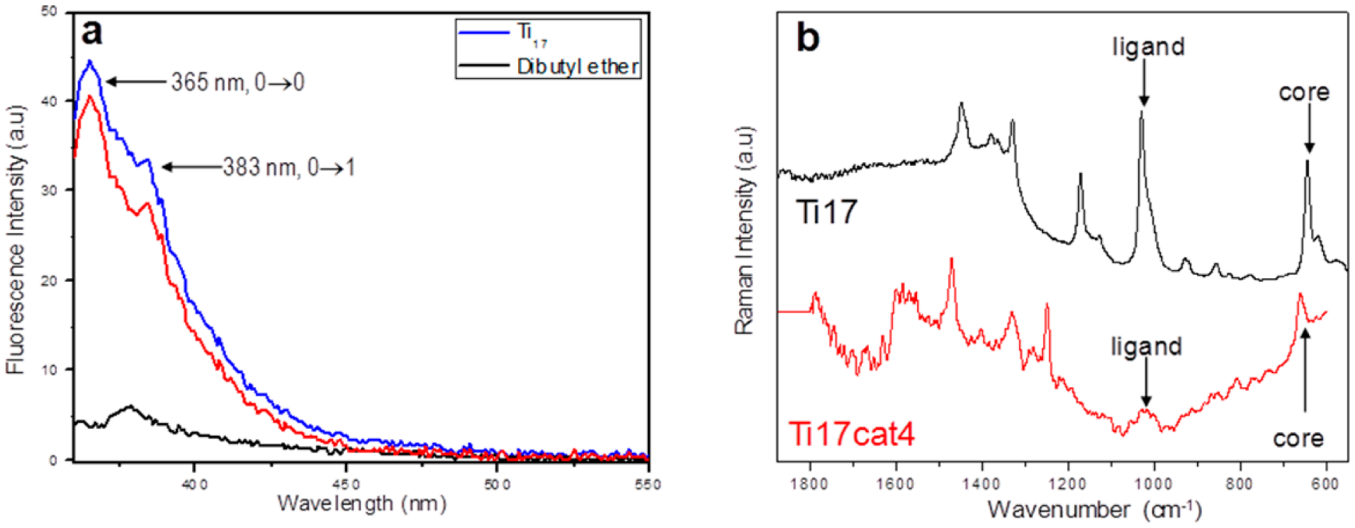

Figure 6. (a) Room temperature fluorescence spectrum of **Ti17** in dibutyl ether showing vibronic bands at 365 and 383 nm (excitation at 340 nm). The spectrum corrected for the solvent background is shown in red. (b) Raman spectrum of solid **Ti17** showing at 1029 cm^{-1} a prominent C−O stretch/CH wagging combination mode of the four isopropoxide ligands bound to the pentacoordinate Ti sites (black) and the corresponding Raman spectrum of solid **Ti17cat** (red), in which the peak corresponding to the C−O stretch of the isopropoxides bound to the five coordinate Ti centers is absent.

exciton recombination dynamics as a slow decay channel which should appear in the time-resolved transient absorption experiments.

The issue of the electron−hole exchange interaction and the resulting singlet−triplet splitting is of great importance for quantum confinement effects at the smallest particle size limit. One should note that the size dependent position of the triplet state in the band gap or HOMO−LUMO gap of the species has implications for the emission efficiency of quantum dots, as well as the multiple exciton generation (MEG)[35] and singlet fission (SF)[36] processes which have been attracting a lot of attention recently because of their potential importance for solar energy conversion. Both phenomena critically depend on the spacing between the energy levels which participate in the partitioning of the initial excitation. The possibility of using the size and shape of the particle to control the electron−hole exchange interaction[29,37] and hence being able to place the triplet exciton at an arbitrary position within the band gap opens attractive possibilities for the design of light conversion materials. We plan to address the possible involvement of triplet excitons in the photophysics of **Ti17** by low temperature luminescence and transient absorption studies.

Fluorescence and Raman Spectra of Ti17: The Involvement of High-Frequency Ligand Modes. **Ti17** exhibits a UV fluorescence band peaking at 365 nm. The emission is broad and extends into the violet portion of the visible spectral range. Although the emission is weak, $\Phi \leq 1\%$, it can be readily measured even at room temperature (Figure 6a). This finding is significant because it provides additional valuable information about the electronic structure of the cluster. The position of the maximum at 365 nm is in perfect agreement with the indirect band gap of 3.36 eV deduced by Benedict and Coppens on the basis of their analysis of the absorption onset of **Ti17**.[7] Furthermore, the fluorescence band shows two discernible vibronic peaks separated by approximately 1290 ± 150 cm^{-1}. The coupling between the emissive exciton and the high frequency promoting mode offers hints about the charge localization in the fully relaxed excited state.

The brookite-like vibrational spectrum of the TiO core of the cluster is similar to those of the bulk phases of TiO_2 (Table 1 and Figure 6b) with a peak at a frequency of 644 cm^{-1}, i.e., much lower than the separation of the vibronic shoulders in the fluorescence spectrum. Therefore, it is doubtful that the vibronic structure of the fluorescence spectrum results from the coupling between the exciton and the core modes of the cluster. The involvement of the ligand modes at the organic−inorganic interface seems much more likely. Indeed, the ground state Raman spectrum of solid **Ti17** shows a very prominent composite peak at 1030 cm^{-1} and another one at 1190 cm^{-1} (Figure 6b) which correspond to the combination CO stretching and CH wagging modes of the isopropoxide ligands[38,39] forming the organic shell of the cluster. We believe that the CO modes are responsible for the vibrational structure of the fluorescence band. If this hypothesis is correct, it would suggest at least one of the charges, most likely the hole of the relaxed exciton, is localized at the core−ligand interface, where it couples to the vibrations of the isopropoxide group.

Very interestingly, the CO Raman bands of **Ti17** originate almost exclusively from four ligands bound to the penta-coordinate Ti sites at the corners of the cluster. As it is depicted in Figure 1b and discussed in the Introduction, the cluster contains four five-coordinate and as a result coordinatively unsaturated Ti centers (shown in green) which are terminated with a single, strongly polarized isopropoxide ligand. Benedict and Coppens found that, upon selective substitution of the five-coordinate Ti centers with bidentate catechol, all surface titanium sites of the resulting **Ti17cat4** cluster (proper name $Ti_{17}(\mu_4\text{-}O)_4(\mu_3\text{-}O)_{16}(\mu_2\text{-}O)_4(cat)_4(OPr^i)_{16}$) become hexa-coordinate.[7] Our results show that upon this substitution the strong CO band nearly completely disappears from the Raman spectrum (Figure 6b), despite the fact that there are still 16 isopropoxide ligands which remain bound to the surface of the core. The explanation for this puzzling observation lies in the degree of the purely ionic vs charge-transfer bonding interaction between the ligand and the surface titanium centers. The CO modes of the closed-shell free isopropoxide ion are strong IR absorbers; however, because of the localized "hard"

dx.doi.org/10.1021/jp307724v | J. Phys. Chem. B 2013, 117, 4422−4430

charge distribution, they are weak Raman scatterers. This is illustrated by the calculated Raman and IR spectra shown in Figure 7. On the contrary, the same vibrational modes of the

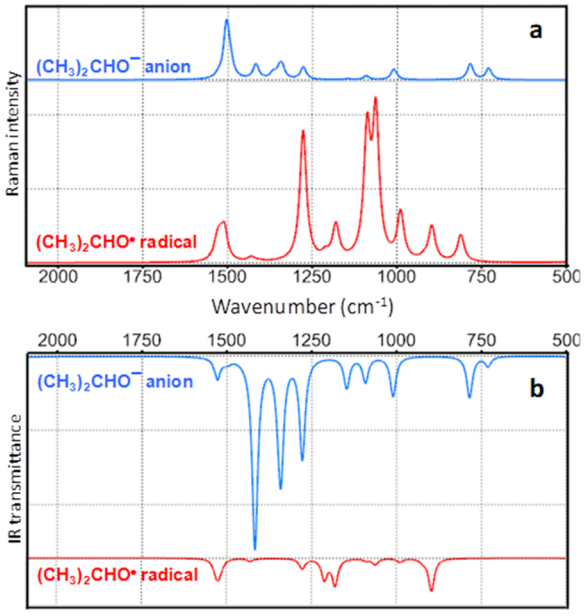

Figure 7. Calculated Raman (a) and IR (b) spectra of the isopropoxide anion (blue) and the oxo isopropoxyl radical (red). Calculations were performed at the B3LYP DFT level (Spartan'10) without frequency scaling.

corresponding open-shell electroneutral oxo-radical are weak IR absorbers in the 750−1500 cm^{-1} region; however, they have much larger Raman cross sections (Figure 7, shown in red). This implies that any shift of electron density from the isopropoxide anion onto the metal center will give rise to stronger Raman scattering in the CO region. It appears that isopropoxides bound to the hexa-coordinate Ti centers retain their primarily ionic character and that there is little charge shift between their oxygen atoms and the d-orbitals of the metal. As a result, they make only a minor contribution to the CO region of the Raman spectrum of **Ti17**. On the other hand, isopropoxides bound to the penta-coordinate Ti centers donate a large fraction of their charge to the d-orbitals of the titanium ions. Such electron density shift renders them considerably less ionic and increases the overall polarizability of the local −C−O−Ti− interface, leading to a strong Raman signature.[40] In inorganic chemistry literature, this type of charge-transfer interaction is often referred to as "π-bonding".[41]

On the basis of the presented fluorescence and Raman data alone, it is not possible to unequivocally decide whether the hole in the excited state of **Ti17** becomes localized on one of the coordinatively unsaturated five-coordinate titanium centers or on one of the more numerous six-coordinate sites. High level calculations on the complete cluster will be necessary in order to settle this question. Nevertheless, it is safe to conclude that ligand modes at the interface play a more significant role in stabilizing the lowest electronic excited state of the **Ti17** cluster than either the solvent reorganization or the core frequencies. This further bolsters the picture of a CT excited state with the hole localized at the core−ligand interface and the electron on the central tetrahedral titanium ion. The implications of the large ground state ligand-to-metal charge shift at the five-coordinate centers, which is so strikingly evident in the Raman spectra, extend beyond the excited state dynamics of **Ti17**. Because of the charge shift, these sites behave as reactive "hot-spots" on the surface of the cluster and for this reason the ligand substitution reactions occur with high selectivity only at these Ti centers. The charge shift must also have an influence on the redox and potential catalytic activity of the cluster both in the ground and in the excited state.

CONCLUSIONS

The 1 nm diameter $Ti_{17}(\mu_4\text{-}O)_4(\mu_3\text{-}O)_{16}(\mu_2\text{-}O)_4(OPr^i)_{20}$ polyoxotitanate cluster with a brookite-like core displays complex photophysics which combines primarily molecular characteristics with some traits typical of larger nanoparticles and bulk TiO_2. The high frequency modes at the ligand−core interface were found to play a key role in the stabilization and localization of the excited state. On the basis of our results, we proposed a tentative energy level diagram of the cluster (Figure 2). Due to spatial confinement, the absorption spectrum of the D_0 ground state of the **Ti17**$^{\bullet-}$ radical anion is shifted from the IR range typical of the excess electron in bulk II−VI oxides[17,25,42] to 1000 nm. The spectrum of the S_1 excited state of the cluster is blue-shifted even further, indicating the presence of large Coulomb and exchange interactions between the spatially confined electron and hole. The appearance of the broad and featureless spectra of the S_1 and D_0 states of **Ti17** is consistent with band-like progressions of closely lying upper electronic states, S_n and D_n, respectively. It is likely that the higher states involve primarily the TiO core of **Ti17** and therefore are of more bulk-like character than the lowest states. DFT calculations show a large Ti d-orbital contribution to low-lying empty orbitals of the cluster, suggesting that the S_1 and D_1 spectra of **Ti17** may be due to d−d transitions.

The electron−hole recombination in **Ti17** is faster than in colloidal anatase or mesoporous films of TiO_2; however, it does not follow single exponential decay. The fast, 0.7−5 ps components, which account for ∼60% of the decay, most likely originate from the recombination of the initial excitons before they relax and become stabilized at the core−ligand interface. The slower, 100 ps component is assigned to the decay of the fully relaxed exciton. Lastly, we consistently detected a long-lived component accounting for 5−10% of the initial population which we tentatively ascribe to the formation of a lower-lying triplet state with a distinct, slower recombination dynamics.

Our findings suggest that the relaxed excited state of **Ti17** has charge transfer character, with one of the charges (hole) localized at the core−ligand interface and the other on the unique tetrahedral Ti at the center of the cluster. The vibronic features of the emission spectrum as well as the ground state Raman spectra show that the ligand modes are strongly coupled to the overall electron density of the cluster. Polyoxometalates and colloidal TiO_2 have been successfully employed in a number of photocatalytic reactions,[5,6] and there are indications that the brookite phase possesses more reactive surface sites than either anatase or rutile.[43,44] A better understanding of the localization and dynamics of electrons and holes in clusters similar to **Ti17** should facilitate further development of catalytic applications of this class of materials.

The authors hope that the presented data will stimulate high-level quantum mechanical calculations, which are necessary for a conclusive interpretation of the experimental results, especially when it comes to the orientation of the transition dipole, the electron and hole localization sites, as well as the

dx.doi.org/10.1021/jp307724v | J. Phys. Chem. B 2013, 117, 4422−4430

magnitude of the Coulomb and exchange interaction in the excited state of **Ti17**. Transient absorption depolarization measurements in the <500 fs window will be used to probe the earliest steps of **Ti17*** relaxation dynamics. Low temperature photoluminescence experiments will be performed to better resolve the vibronic structure of the fluorescence spectrum of **Ti17** and to search for the phosphorescence spectrum of the ^{3}**Ti17*** triplet state.

AUTHOR INFORMATION

Corresponding Author

*E-mail: piotr@andromeda.rutgers.edu.

Notes

The authors declare no competing financial interest.

ACKNOWLEDGMENTS

The work at Rutgers University was supported by Division of Chemical Sciences, Geosciences, and Biosciences, Office of Basic Energy Sciences of the U.S. Department of Energy through Grant No. DE-FG02-06ER15828 to P.P. The work at University at Buffalo was funded by the Division of Chemical Sciences, Geosciences, and Biosciences, Office of Basic Energy Sciences of the U.S. Department of Energy through Grant DE-FG02-02ER15372 to P.C. The femtosecond laser instrumentation used to carry out this research was funded by National Science Foundation CRIF Grant No. 0342432 to P.P. The authors gratefully acknowledge support of the Division of Chemical Sciences, Geosciences, and Biosciences, Office of Basic Energy Sciences of the U.S. Department of Energy through Grant No. DE-AC02-98-CH10886 to all authors, and for use of the LEAF Facility of the BNL Accelerator Center for Energy Research. We are grateful to Prof. Richard Mendelsohn for the help with the Raman measurements, Prof. Frieder Jaekle for the access to one of his glove boxes, and Prof. Galoppini for the loan of the spectro-electrochemistry setup. We thank Prof. Victor Batista and his group for sharing with us their computational results on the related **Ti17cat4** polyoxotitanate cluster.

REFERENCES

(1) Alivisatos, A. P.; Harris, A. L.; Levinos, N. J.; Steigerwald, M. L.; Brus, L. E. *J. Chem. Phys.* **1988**, *89*, 4001−4011.
(2) Brus, L. *J. Phys. Chem.* **1986**, *90*, 2555−2560.
(3) Brus, L. E. *J. Chem. Phys.* **1983**, *79*, 5566−5571.
(4) Brus, L. E. *J. Chem. Phys.* **1984**, *80*, 4403−4409.
(5) Pope, M. T.; Achim, M. *Polyoxometalates: from platonic solids to anti-retroviral activity*; Kluwer Academic Publishers: Dordrecht, The Netherlands, 1994.
(6) Duncan, D. C.; Netzel, T. L.; Hill, C. L. *Inorg. Chem.* **1995**, *34*, 4640−4646.
(7) Benedict, J. B.; Coppens, P. *J. Am. Chem. Soc.* **2010**, *132*, 2938−2944.
(8) Benedict, J. B.; Freindorf, R.; Trzop, E.; Cogswell, J.; Coppens, P. *J. Am. Chem. Soc.* **2010**, *132*, 13669−13671.
(9) Ardo, S.; Meyer, G. J. *Chem. Soc. Rev.* **2009**, *38*, 115−164.
(10) Fujishima, A.; Honda, K. *Nature* **1972**, *238*, 37−38.
(11) Linsebigler, A. L.; Lu, G. Q.; Yates, J. T. *Chem. Rev.* **1995**, *95*, 735−758.
(12) Amtout, A.; Leonelli, R. *Phys. Rev. B* **1995**, *51*, 6842−6851.
(13) Gonzalez, R. J.; Zallen, R.; Berger, H. *Phys. Rev. B* **1997**, *55*, 7014−7017.
(14) Lottici, P. P.; Bersani, D.; Braghini, M.; Montenero, A. *J. Mater. Sci.* **1993**, *28*, 177−183.
(15) Martin, S. T.; Herrmann, H.; Hoffmann, M. R. *J. Chem. Soc., Faraday Trans.* **1994**, *90*, 3323−3330.
(16) Mattsson, A.; Osterlund, L. *J. Phys. Chem. C* **2010**, *114*, 14121−14132.
(17) Yamakata, A.; Ishibashi, T.; Onishi, H. *Chem. Phys. Lett.* **2001**, *333*, 271−277.
(18) Chiodo, L.; Garcia-Lastra, J. M.; Iacomino, A.; Ossicini, S.; Zhao, J.; Petek, H.; Rubio, A. *Phys. Rev. B* **2010**, 82.
(19) Hendry, E.; Wang, F.; Shan, J.; Heinz, T. F.; Bonn, M. *Phys. Rev. B: Condens. Matter Mater. Phys.* **2004**, 69.
(20) Serpone, N.; Khairutdinovt, D. L. a. R. *J. Phys. Chem.* **1995**, *99*, 16646−16654.
(21) Steunou, N.; Kickelbick, G.; Boubekeur, K.; Sanchez, C. M. *J. Chem. Soc., Dalton Trans.* **1999**, 3653−3655.
(22) Steunou, N.; Portal, R.; Sanchez, C. *High Pressure Res.* **2001**, *20*, 63−70.
(23) Ernstorfer, R.; Gundlach, L.; Felber, S.; Storck, W.; Eichberger, R.; Willig, F. *J. Phys. Chem. B* **2006**, *110*, 25383−25391.
(24) Wishart, J. F.; Cook, A. R.; Miller, J. R. *Rev. Sci. Instrum.* **2004**, *75*, 4359−4366.
(25) Yoshihara, T.; Katoh, R.; Furube, A.; Tamaki, Y.; Murai, M.; Hara, K.; Murata, S.; Arakawa, H.; Tachiya, M. *J. Phys. Chem. B* **2004**, *108*, 3817−3823.
(26) Schmuttenmaer, C. Personal communication.
(27) Skinner, D. E.; Colombo, D. P.; Cavaleri, J. J.; Bowman, R. M. *J. Phys. Chem.* **1995**, *99*, 7853−7856.
(28) Wang, L. W.; Zunger, A. *Phys. Rev. Lett.* **1994**, *73*, 1039−1042.
(29) Takagahara, T. *Phys. Rev. B* **1993**, *47*, 4569.
(30) Scholes, G. D. *ACS Nano* **2008**, *2*, 523−537.
(31) Scholes, G. D.; Rumbles, G. *Nat. Mater.* **2006**, *5*, 683−696.
(32) Hörmann, U.; Kaiser, U.; Albrecht, M.; Geserick, J.; Hüsing, N. *J. Phys.: Conf. Ser.* **2010**, *209*, 012039.
(33) Arbogast, J. W.; Darmanyan, A. P.; Foote, C. S.; Rubin, Y.; Diederich, F. N.; Alvarez, M. M.; Anz, S. J.; Whetten, R. L. *J. Phys. Chem.* **1991**, *95*, 11−12.
(34) Foote, C. Photophysical and photochemical properties of fullerenes. In *Top. Curr. Chem.*; Mattay, J., Ed.; Springer-Verlag: Berlin/Heidelberg, 1994; Vol. *169*, pp 347−363.
(35) Stewart, J. T.; Padilha, L. A.; Qazilbash, M. M.; Pietryga, J. M.; Midgett, A. G.; Luther, J. M.; Beard, M. C.; Nozik, A. J.; Klimov, V. I. *Nano Lett.* **2012**, *12*, 622−628.
(36) Schwerin, A. F.; Johnson, J. C.; Smith, M. B.; Sreearunothai, P.; Popovic, D.; Cerny, J.; Havlas, Z.; Paci, I.; Akdag, A.; MacLeod, M. K.; et al. *J. Phys. Chem. A* **2010**, *114*, 1457−1473.
(37) Brovelli, S.; Schaller, R. D.; Crooker, S. A.; García-Santamaría, F.; Chen, Y.; Viswanatha, R.; Hollingsworth, J. A.; Htoon, H.; Klimov, V. I. *Nat. Commun.* **2011**, *2*, 1−8.
(38) Bell, J. V.; Heisler, J.; Tannenbaum, H.; Goldenson, J. *Anal. Chem.* **1953**, *25*, 1720−1724.
(39) Lynch, C. T.; Mazdiyasni, K. S.; Smith, J. S.; Crawford, W. J. *Anal. Chem.* **1964**, *36*, 2332−2337.
(40) Moran, P. D.; Bowmaker, G. A.; Cooney, R. P.; Finnie, K. S.; Bartlett, J. R.; Woolfrey, J. L. *Inorg. Chem.* **1998**, *37*, 2741−2748.
(41) Chisholm, M. H.; Davidson, E. R.; Huffman, J. C.; Quinlan, K. B. *J. Am. Chem. Soc.* **2001**, *123*, 9652−9664.
(42) Yoshihara, T.; Katoh, R.; Furube, A.; Murai, M.; Tamaki, Y.; Hara, K.; Murata, S.; Arakawa, H.; Tachiya, M. *J. Phys. Chem. B* **2004**, *108*, 2643−2647.
(43) Koelsch, M.; Cassaignon, S.; Guillemoles, J. F.; Jolivet, J. R. *Thin Solid Films* **2002**, *403*, 312−319.
(44) Lin, H. F.; Li, L. P.; Zhao, M. L.; Huang, X. S.; Chen, X. M.; Li, G. S.; Yu, R. C. *J. Am. Chem. Soc.* **2012**, *134*, 8328−8331.